CHAPTER 138

DEFORMATION OF TIDAL WAVES IN SHALLOW ESTUARIES

by

CLAUDE MARCHE[1] and HANS-WERNER PARTENSCKY[2]

ABSTRACT

Several mathematical models have been lately presented which describe the tidal wave propagation within an estuary. The existing models derived from the method for damped co-oscillating tides are based on sinusoidal wave profile.

Meanwhile a tidal wave which moves upstream, generally exhibits a progressive deformation which tends to unbalance the length of time between flood and ebb tides. The actual profile is therefore no longer sinusoidal.

Our investigation uses the potential method, and takes into account the wave amplitude which is usually neglected compared with the water depth.

Finally, the velocity potential is obtained explicitely, using a double iterative method. Tidal elevation, particle velocities and trajectories are given by the same computer programmed algorithm.

Our study shows that 1) the phenomenon can be clearly visualized on the theoretical curves and 2) the magnitude of this deformation is inversely proportional to the water depth, becoming significant when the ratio η/h reaches the critical value of $1/10$.

Damping and geometrical effects are also considered and the theory was applied to the St.Lawrence Estuary. A partial positive reflection of the incoming tidal wave is assumed at the narrow section near Quebec, whereas a complete negative reflection is assumed at the entrance to Lake St.Peter. The calculated and observed wave profiles, velocity distributions, and phase shifts are in good agreement.

I. INTRODUCTION

Several mathematical models have been developped, describing the tidal wave propagation in an estuary. The existing models, for-mulated by A.T. Ippen and D.R.F. Harleman, for the Delaware Estuary and the Bay of Fundy [1], as well as that of H.W. Partenscky for the St.Lawrence Estuary [2,3], made use of the method for damped co-oscillating tide, based on a sinusoidal wave profile.

---

1) Lecturer, Ecole Polytechnique, Montreal, Canada.
2) Director, Franzius Institute, Technical University of Hannover, Germany.

However, a tidal wave ascending an estuary, generally under-goes a progressive deformation which tends to unbalance the respective ebb and flood times of the water mass. The actual profile is therefore no longer sinusoidal.The theory,developped in this paper, allows us to explain and retrace this wave deformation, by taking the influence of the water depth into account.

II. DEFORMATION OF TIDAL WAVE IN A SHALLOW RECTANGULAR CHANNEL

   1. Velocity potential and free surface elevation

        The velocity potential of an oscillating wave of small ampli-tude propagating in the positive x direction is solution of the Laplace equation

$$\nabla^2 \; \phi_1 \; = \; 0$$
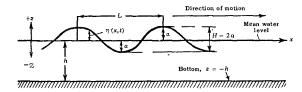
where index 1 indicates the incident wave.

Fig. 1: Definition sketch

We consider the hypothesis of the small amplitude wave theory verified; however, we locate the free surface at elevation $z = \eta_1$, variable, and not at the mean elevation $z = 0$. The boundary conditions to be used to evaluate the resulting solution are:

at $z = \eta_1$:

$$- \frac{\partial \phi_1}{\partial t} + \frac{1}{2} \left(\frac{\partial \phi_1^2}{\partial x} + \frac{\partial \phi_1^2}{\partial y} \right) + g \, \eta_1 \; = \; 0$$

$$- \frac{\partial \eta_1}{\partial t} + \frac{\partial \phi_1}{\partial x} \cdot \frac{\partial \eta_1}{\partial x} - \frac{\partial \phi_1}{\partial z} \; = \; 0 \qquad\qquad (1)$$

at $z = - h$:

$$\frac{\partial \phi_1}{\partial z} \; = \; 0$$

By neglecting the higher order terms, the boundary conditions can be written in a simplified form:

at $z = \eta_1$:

$$- \frac{\partial \emptyset_1}{\partial t} + g \, \eta_1 = 0$$

$$- \frac{\partial \eta_1}{\partial t} - \frac{\partial \emptyset_1}{\partial z} = 0 \tag{2}$$

at $z = -h$:

$$\frac{\partial \emptyset_1}{\partial z} = 0$$

We note that the boundary conditions (2) differ from the usual conditions for waves of small amplitude by an order of approximation. This leads us to assume as a first approximation an initial solution of the form:

$$\emptyset_1 = \frac{ag}{\sigma} \frac{\cosh G_1 (h+z)}{\cosh G_1 h} \cos(G_1 x - \sigma t) = \frac{A_1 g}{\sigma} \cos(G_1 x - \sigma t) \tag{3}$$

The boundary conditions (2) will now be applied to the velocity potential function $\emptyset_1$. Solution (3) fulfills the boundary conditions if

$$\sigma^2 = g \, G_1 \, \tanh G_1 (h + \eta_1) \tag{4}$$

is verified. In the above equations, a is the amplitude of the tidal wave, η_1 is the instantaneous surface elevation given by

$$\eta_1 = \frac{1}{g} \frac{\partial \emptyset_1}{\partial t} \quad \text{and} \quad G_1 = \frac{2\pi}{L_1}$$

is the variable wave number.

It should be stressed the importance of equation (4) which shows that σ and G_1 are related by a variable expression depending on the elevation η_1, the latter being a function of time and space. Field measurements have shown the rigourous equality of the period of different tidal waves. This verification allows us to present the third equation needed:

$$\sigma = \frac{2\pi}{T} = \text{constant}$$

Equation (4) is an implicit equation in G_1, and an iterative computer programmed method will yield to a numerical solution in the system formed by equations (3) and (4). The uniqueness of the solution of this system is proved for all possible physical conditions. The deformation clearly appears when a comparison is made between the wave profile

obtained from this theory and the sinusoidal profile.

Figure 2 illustrates the type of deformation which a five feet amplitude wave undergoes, during propagation in a channel of fifteen   feet depth. We note in particular a descending time of six tenth (6/10) period versus an ascending time of four tenth (4/10) of a period. Several similar curves, calculated for different water depths showed that the importance of the deformation becomes appreciable for a ratio of amplitude to depth of

$$\eta/h > 1/10$$

approximately.

The application of this theory to the potential of a wave reflected at x = B in the same rectangular channel leads to the following expression, with index 2 being used for the reflected wave:

$$\emptyset_2 = \frac{ag}{\sigma} \frac{\cosh G_2 (h+z)}{\cosh G_2 h} \cos(G_2 x - \sigma t + \delta) = \frac{A_2 g}{\sigma} \cos(G_2 x - \sigma t + \delta) \quad (5)$$

with:
$$G_2 = \frac{2\pi}{L_2}$$

$$\sigma = g G_2 \tanh G_2 (h + \eta_2)$$

and
$$\delta = 2 n\pi - 2 G_2 B$$

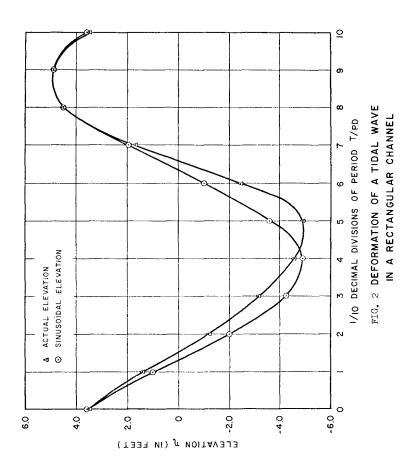The velocity potential of the resulting wave is given by

$$\Phi = \emptyset_1 + \varkappa_r \emptyset_2 \qquad (6)$$

where $\varkappa_r$ is the reflection coefficient of the reflected wave at x = B.

2. Introduction of   geometry and damping effects

The generalization of this theory to a practical application requires the introduction of two additional parameters: geometry and friction. In the most general case, the resulting wave profile is given by the expression

$$\eta = a\left(\frac{b_B}{b_x}\right)^{\frac{1}{2}} \left(\frac{h_B}{h_x}\right)^{\frac{1}{4}} \left[A_1 e^{-\mu(x-B)} \sin(G_1 x - \sigma t) - \varkappa_r A_2 e^{\mu(x-B)} \sin(G_2 x - \sigma t + \delta)\right] \quad (7)$$

FIG. 2 DEFORMATION OF A TIDAL WAVE IN A RECTANGULAR CHANNEL

with the supplementary condition:

$$\sigma^2 = g\, G_1\; \tanh G_1\,(h + \eta_1) = g\, G_2\; \tanh G_2\,(h + \eta_2) \qquad (8)$$

where:

    h is the mean water depth
    b is the mean width
    h is the overall damping coefficient
    A_1 and A_2 are terms as defined in equations (3) and (5) respectively

Expression (7) is valid and may be used for any real estuary, with the condition that Green's Law be satisfied.

3. Water particle velocity

By virtue of the definition of the velocity potential, the horizontal and vertical components of a local fluid particle velocity due to the passage of the incident wave in a rectangular channel without friction are obtained by differentiation of the velocity potential in each direction:

$$U = -\frac{\partial \phi_1}{\partial x} = \frac{ag\, G_1}{\sigma}\; \frac{\cosh G_1\,(h + \eta_1)}{\cosh G_1\, h}\; \sin(G_1\, x - \sigma t) \qquad (9)$$

$$V = -\frac{\partial \phi_1}{\partial z} = -\frac{ag\, G_1}{\sigma}\; \frac{\sinh G_1\,(h + z)}{\cosh G_1\, h}\; \cos(G_1\, x - \sigma t) \qquad (10)$$

The implicit equation

$$\sigma^2 = g\, G_1\, \tanh G_1\,(h + \eta_1)$$

defining the term $G_1 = 2\pi/L_1$ used in the expressions (9) and (10). A numerical solution is utilized to determine the velocity components U and V as functions of x and z. Figure (3) shows a characteristic variation of the horizontal velocity during a wave period. We note from this curve a difference between the absolute values of minimum (5.20 feet/sec) and maximum (4.15 feet/sec) velocity of the particle considered: The velocity of reflux is of greater importance than the velocity of flux.

Therefore, for incompressible, two dimensional motion in the x, z plane the continuity equation requires that the corresponding period of time of rise and fall be unequal. This last observation corroborates

FIG. 3 HORIZONTAL VELOCITY CHANGE DURING A PERIOD

the mathematical and physical results concerning the tidal elevation, shown on figure (2).

4. Water particle trajectories

Another modification of importance given by this theory concerns the trajectories of particles. These are solution of the differential system

$$\frac{dx}{U} = \frac{dz}{V} = dt \qquad (11)$$

In the integration of this system, we do not use the small particle movement hypothesis, thus allowing us to consider that particle velocity is only a time fonction. The complete integration of the system (11) may be made numerically, and without particular hypothesis, and leads to the following algorithm:

$$x_{t_n} = \sum_{n=1}^{n} \int_{(n-1)\frac{T}{m}}^{n\frac{T}{m}} U(x_{n-1}, t_{n-1})dt + x_0 \qquad (12)$$

$$z_{t_n} = \sum_{n=1}^{n} \int_{(n-1)\frac{T}{m}}^{n\frac{T}{m}} W(x_{n-1}, t_{n-1})dt + z_0 \qquad (13)$$

where:

x_{t_n} and z_{t_n} are the instantaneous horizontal and vertical displacements from 0 to t_n respectively and,

T/m is the increment of the numerical solution expressed as a fraction of the period.

Figure (4) illustrates the trajectory of a particle under the effect of a wave propagating in a very shallow region. We note that the initial ellipse obtained from the small amplitude wave theory is downward deformed.
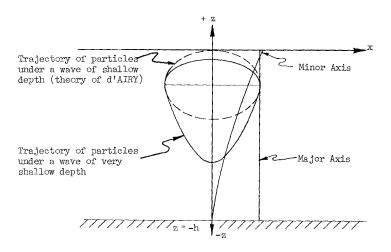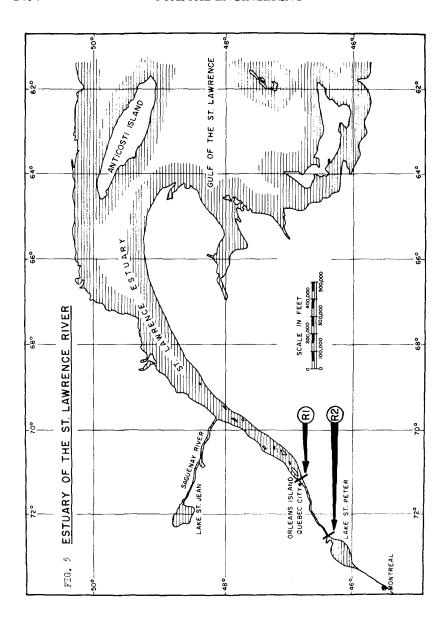
Figure 4

This deformation is easily explained by continuity by observing the velocity differences of flux and reflux. The calculated trajectories for different water depths show that there exists a variation in trajectory comparable to the well-known variation of ellipses in small amplitude wave theory. The major axis of the deformed ellipse remains constant at any depth, whereas the minor axis, in the vertical direction decreases with depth.

III. APPLICATION OF THE THEORY TO THE ST. LAWRENCE ESTUARY

1. Physical characteristics of the estuary

The St. Lawrence Estuary is composed of two parts of different geometry. The first concerning the estuary itself is a convergent form between its ocean entry and Quebec City. It is prolongated by a second part of more constant width and far shallower depths, bounded at the location of the enlargement known as Lake St. Peter.

FIG. 5 ESTUARY OF THE ST. LAWRENCE RIVER

SCALE IN FEET

ANTICOSTI ISLAND

GULF OF THE ST. LAWRENCE

ESTUARY

ST. LAWRENCE

SAGUENAY RIVER

LAKE ST. JEAN

ORLEANS ISLAND

QUEBEC CITY

R1

R2

LAKE ST. PETER

MONTREAL

These two distinct parts of the estuary, bring us to consider two successive reflexions of the ascending tidal wave: one partically positive at the straightening of Quebec (Section R_1), the other total and negative, at the sudden enlargement at Lake St. Peter (Section R_2).

2. Results

Some physical parameters are required for the solution of the actual conditions in the estuary. These are:

- The reflection and transmission coefficients particularly in the sections R_1 and R_2. These are furnished by a geometric study in that sector.

- The height of the tidal wave in the sections of reflection. These are found in the bibliography.

- The precise geometry of the estuary, the surface width and the average depth of each section under study.

Based on these informations, the application of the mathematical model allows us to predict the tidal elevation, the particle velocity and their trajectory at each section of the estuary, the instantaneous wave profile and the velocity distributions along the estuary at any time.

A comparison of the recorded and calculated elevations at the tidal stations of Neuville and Grondine (figure 5), which are located at the upper shallower part of the estuary, is shown on figure 6 and 7. These curves show the expected deviation from the pure sinusoidal motion due to the restricted water depth in this region. In the deeper part of the estuary, the graphs of $\eta(t)$ regain a more sinusoidal form.

Figure 8 presents the variation of the horizontal velocity of the particles at three sections of the upper part of the estuary: Neuville, Grondines, and Batiscan. We note from these three curves a difference between the absolute value of minimum and maximum velocities, which is proportional to the maximum velocity itself.

Figure 9 shows the trajectory of a particle initially located at Grondines and at a distance of seven feet above the bottom. We note that since the displacement is a periodic function of time in the expressions (12) and (13), the trajectories are closed curves. For comparison, the trajectory of a particle initially located at Batiscan above Grondines is shown on the same figure. We note that the conjugated effects of the damping and the geometry of the estuary tend to reduce the particle displacement in accordance with the wave propagation. In the deeper part of the estuary the trajectories appear elliptic.
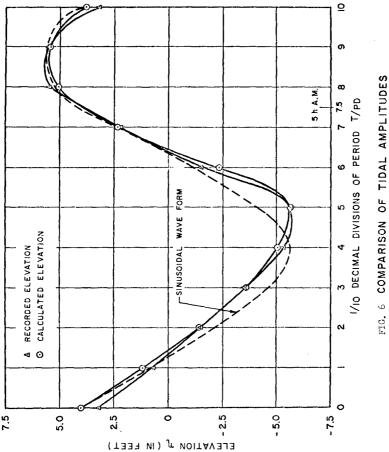
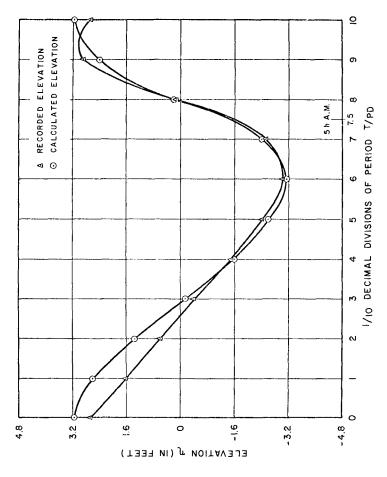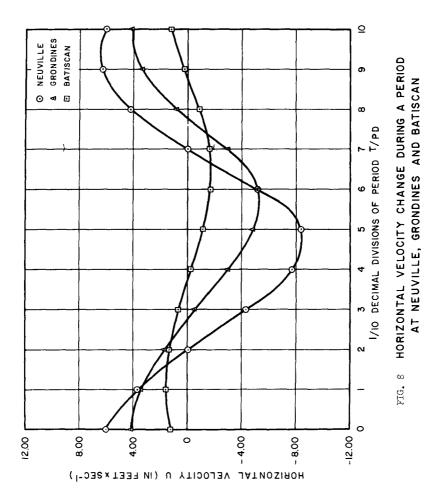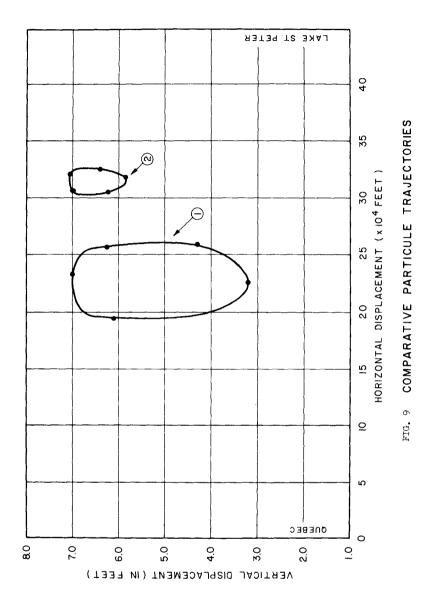FIG. 6 COMPARISON OF TIDAL AMPLITUDES RECORDED AND CALCULATED AT NEUVILLE

FIG. 7 COMPARISON OF TIDAL AMPLITUDES
RECORDED AND CALCULATED AT GRONDINES

FIG. 8   HORIZONTAL VELOCITY CHANGE DURING A PERIOD
          AT NEUVILLE, GRONDINES AND BATISCAN

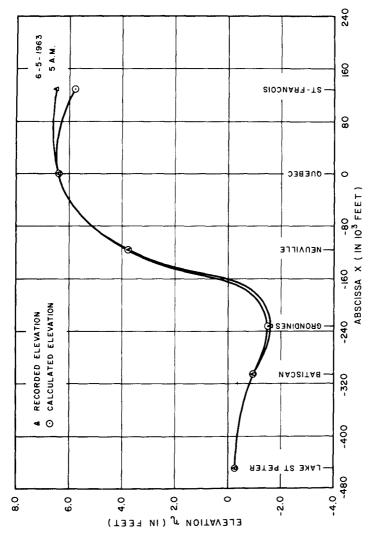FIG. 9 COMPARATIVE PARTICULE TRAJECTORIES

FIG. 10 INSTANTANEOUS PROFILE ALONG THE ESTUARY BETWEEN ST-FRANCOIS AND LAKE ST PETER

An instantaneous profile calculated for the upper part of the estuary is shown in figure 10. The calculation was made for 5 A.M. on May 5, 1963, a date for which a detailed recording was available. A comparison with the recorded data shows the accuracy of the theoretical values of the tidal elevations. On the other hand, these curves clearly show the effect of the total negative reflection of a tidal wave and its decline in the upper part of the estuary.

CONCLUSION

The mathematical model herein developped and applied to the St. Lawrence Estuary gives a good approximation of the tidal motion in both, the deeper and shallower part of the estuary. Especially in the shallower zone, the results show the well-known deformation of the wave profile which could not be predicted by preceeding mathematical models. The theoretical development used here, allows a computer oriented approach which could be modified to incorporate into the equations some of the more complex aspects of propagation of the tidal wave in an estuary, particularly the effect of the fresh water discharge, which was not yet included in the present study.

BIBLIOGRAPHY

(1) A.T. Ippen &   : "Estuary and Coastline Hydrodynamics", McGraw-Hill,
    D.R.F. Harleman   New York, 1965.

(2) H.W.Partenscky   : "Tidal Motion in the St. Lawrence Estuary", Xth
    & R. Vincent   Conference on Coastal Engineering, Tokyo,
                           Sept. 1966.

(3) H.W. Partenscky   : "A Study of the St. Lawrence River tides estuary
    & J.C. Warmoes   using a linearized mathematical model", Ecole
                           Polytechnique, Montréal.

(4) H.W. Partenscky   : "Damped co-oscillating tides with negative reflec-
    & J.C. Warmoes   tion at the end of the estuary, IAHR, Kyoto, 1969.